Available online at www.sciencedirect.com
ScienceDirect
Journal of the European Ceramic Society 28 (2008) 2693–2699
www.elsevier.com/locate/jeurceramsoc

Processing and properties of a mica–apatite glass–ceramic reinforced with Y-PSZ particles

M. Montazerian [a], P. Alizadeh [a,*], B. Eftekhari Yekta [b]

[a] *School of Engineering, Tarbiat Modares University, Tehran, Iran*
[b] *Ceramic Division, Department of Materials, Iran University of Science and Technology, Tehran, Iran*

Received 5 January 2008; received in revised form 14 April 2008; accepted 18 April 2008
Available online 9 June 2008

Abstract

In this study, mica–apatite glass–ceramic was reinforced with 5, 10 and 15 wt.% partially stabilized zirconia (Y-PSZ). The composites were prepared via pressureless sintering, which was performed on the mixtures of zirconia particulates and two frits belonging to the fluoro-mica and apatite-based glasses. The sintered composites were characterized by scanning electron microscopy (SEM), energy dispersion spectroscopy (EDS) and X-ray diffraction (XRD). Mechanical properties of the sintered samples such as bending strength, Vickers micro-hardness and fracture toughness were also investigated. The results showed that Y-PSZ dissolved in the residual glass and caused the formation of prismatic zircon crystals ($ZrSiO_4$) precipitated during the final stage of sintering. Spherical zirconia particles were also detected. Mechanical properties improved for composite containing 10 wt.% ZrO_2.

Keywords: Glass–ceramics; Composites; Sintering; Mechanical properties; ZrO_2

1. Introduction

Mica–apatite glass–ceramics are well-known bioactive and machinable ceramics, which are extensively used in the human body as an implant. However, these materials suffer from low mechanical strength which has limited their applications in high load-bearing conditions.[1] They can be produced via the controlled nucleation and crystallization of the crystals from the parent glasses.[2,3] The properties of these materials strongly depend on the morphology of the crystalline phases existing in the material.[3] For example, glass–ceramics containing orientated or needle-like apatite represent high strength and fracture toughness,[4,5] and mica crystals with conventional house of cards structure would improve the machinability of these materials.[3] Additionally, mica–apatite glass–ceramics containing calcium mica crystals, demonstrate better mechanical properties.[6]

Zirconia (ZrO_2) is a promising ceramic in medicine because it is nearly inert bioceramic which has high mechanical strength.[7] Additionally, the unique transformation toughening behavior of this material makes it suitable for use as a reinforcing phase in the matrix of composites.[8] ZrO_2 is widely used to reinforce glass or glass–ceramic matrixes.[9–14] The mechanical properties of mica–apatite glass–ceramic (Bioverit® I) have been improved to some extent by Verné et al. through an incorporation of 20 wt.% zirconia particulates into the glass–ceramic matrix.[9] The mechanical strength of glass–ceramics containing apatite-wollastonite, β-spodumene and cordierite crystals has been also successfully improved by ZrO_2 particulates.[10–13] Zirconia has been also employed to reinforce glazes of floor tiles.[14] The reaction between glassy phase and zirconia usually has been reported in these composite systems, and resulted in the formation of zircon ($ZrSiO_4$).[11–14] Verné et al. have conducted pressureless sintering on the mixture of ZrO_2 and crystallized mica–apatite glass, and no reaction between ZrO_2 and crystallized glass powder has been observed.[9] In the apatite-wollastonite glass–ceramic reinforced with ZrO_2, no zircon formation has been reported.[10] In our previous study, in which mica glass–ceramic has been toughened by Y-PSZ, a minor amount of zircon formed due to the dissolution of Y-PSZ in the residual glass, which also caused the transformation of tetragonal zirconia to monoclinic zirconia.[15] In spite of these studies,

* Corresponding author at: School of Engineering, Tarbiat Modares University, P.O. Box 14115-143, Tehran, Iran. Tel.: +98 21 88011001.
E-mail address: p-alizadeh@modares.ac.ir (P. Alizadeh).

0955-2219/$ – see front matter © 2008 Elsevier Ltd. All rights reserved.
doi:10.1016/j.jeurceramsoc.2008.04.022

Table 1
Composition of parent glasses (wt.%)

Glass	SiO_2	CaO	Al_2O_3	MgO	K_2O	F	B_2O_3	P_2O_5	Fe_2O_3
GM	40.13	–	16.24	19.11	8.00	9.55	2.23	4.45	–
GA	29.12	45.35	–	4.30	–	–	–	16.23	5

the influence of glass composition, firing process and fabricating procedures on the zircon formation in glass–ceramic matrix composites containing ZrO_2 is not completely clear yet.

Previous study revealed that pressureless sintering performed on mixtures of apatite-based frit (viz. $CaO–SiO_2–P_2O_5–MgO$ glass system) and a mica-based one, resulted in the formation of mica–apatite and mica-diopside glass–ceramics with appropriate properties.[16] In this study, mica–apatite glass–ceramic, which was fabricated by pressureless sintering of 20 wt.% apatite-based glass and 80 wt.% of a mica-based one, was chosen as a matrix for the composite. Y-PSZ particulate (ZrO_2 partially stabilized with 3 mol% Y_2O_3) was added to the mixture of the two above mentioned frits and pressureless sintering was employed to prepare the composites. Improving the mechanical properties and investigation into the interactions between the two frits and zirconia particles were the objectives of this research.

2. Experimental procedure

2.1. Glass preparation

The chemical compositions of the two glasses are given in Table 1. The GM and GA denote glasses from which the mica and apatite would crystallize, respectively. The raw materials used in the preparation of the glasses were SiO_2, Al_2O_3, $Mg(OH)_2$, K_2CO_3, H_3BO_3, MgF_2, $NH_4H_2PO_4$, $CaCO_3$ and Fe_2O_3, all high quality reagents supplied by Merck. The GM and GA batches were preheated at 900 °C for 1 h and then melted in platinum crucible at 1410 and 1430 °C for 30 min, respectively. The melts were then quenched in cold distilled water to obtain frits. The GM and GA frits were dried and then milled in a high-speed alumina mill in an ethanol media for 45 and 50 min, respectively.

2.2. Preparation of composites

The milled glass powders in a proportion of 80 wt.% GM and 20 wt.% GA were mixed with 5, 10 and 15 wt.% Y-PSZ powder (Aldrich; submicron powder with mean particle size of 0.89 μm). Wet mixing in ethanol was performed for 6 h in an alumina jar-mill. The dried powder of each sample was granulated by adding 2 wt.% polyvinyl alcohol solution. Homogenous and granulated powders were pressed using uniaxial hydraulic press into discs (10 mm in diameter and 4 mm thickness) at the final pressure of 65 MPa. After the organic binder was removed from the samples by holding at 450 °C for 1 h, the samples were fired in the temperature range of 1060–1130 °C, in an electric furnace; at a heating rate of 20 °C/min. Soaking time was 240 min. The composites containing 5, 10 and 15 wt.% Y-PSZ named as C5Z, C10Z and C15Z, respectively.

2.3. Analysis methods

The particle size measurement of the glass powders was carried out by a laser particle size analyzer (Fritsch, Analysette 22). The bulk density of the sintered samples was determined by the Archimedes method. The real density was measured by pycnometery. The crystallized samples were then subjected to XRD analysis using a powder diffractometer (Philips XPert, Cu Kα radiation at 40 kV). Silicon powder was used as the standard for semi-quantitative measurements. The microstructural studies were done by scanning electron microscope (SEM, Philips XL30) equipped with energy dispersive spectroscopy (EDS).

Sintered rectangular bars (2.5 mm × 5 mm × 25 mm) were also used for three-point bending strength and fracture toughness measurements. The flexural strength was determined using a three-point bend fixture with a span of 20 mm. The fracture strength measurements were performed on single edge-notched beam (SENB) specimens with a span of 20 mm, and a nearly half-thickness notch (~2.5 mm) made using a low speed diamond cutting saw (Buehler, Isomet). The notch had a nominal thickness of 0.3 mm. The fracture toughness value was calculated according to ASTM E399. The flexural strength and the fracture toughness tests were conducted in air at room temperature (Instron Universal Testing Machine-1196 machine) with a crosshead speed of 1 mm/min. At least seven specimens were tested for each test condition. A Vickers micro-hardness tester with a diamond pyramid indenter (Buehler, Micromet 1) was used to measure micro-hardness. The load was 500 g and the loading time was 30 s. Data of hardness were determined using at least ten indentations on each polished specimen.

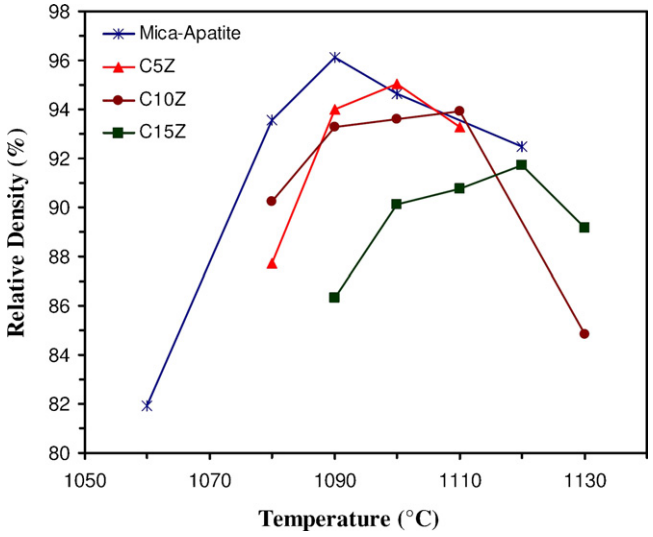

Fig. 1. Relative density of fired samples vs. temperature.

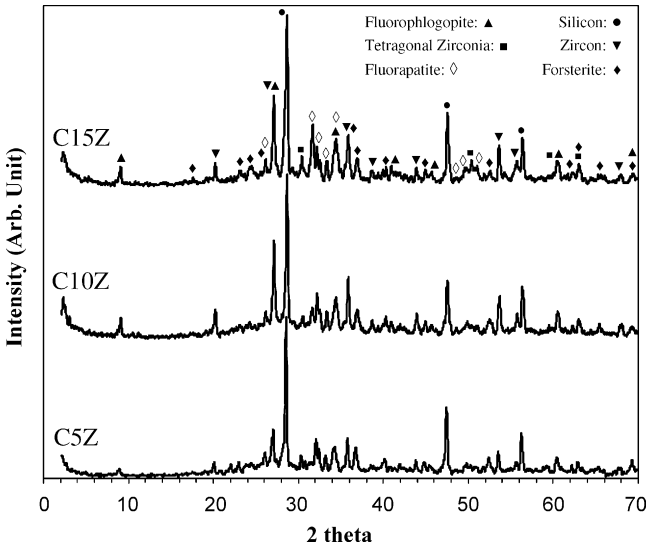

Fig. 2. XRD patterns of composites sintered at optimum sintering temperatures.

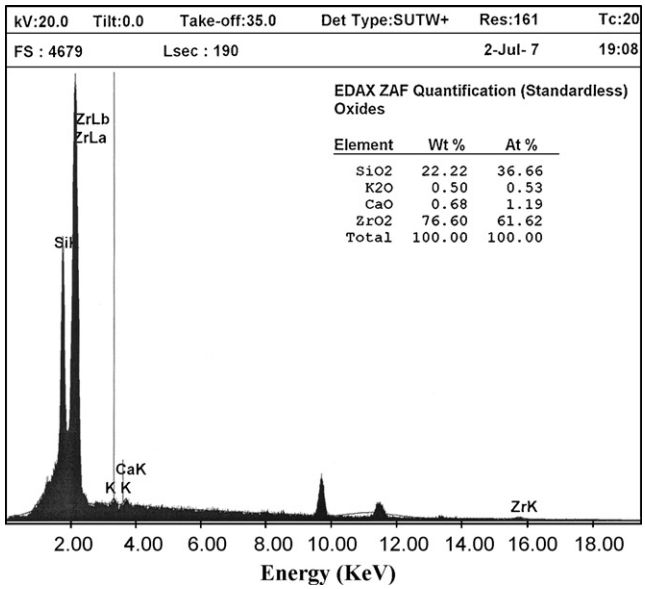

Fig. 4. EDS analysis of prismatic zircon crystal.

3. Results and discussion

The mean particle sizes of the GM and GA as well as their mixture after ball-milling were 12.5, 12.8 and 8.2 μm, respectively. The sinterability and mechanical properties of mica–apatite glass–ceramic prepared via pressureless sintering of 80 wt.% GM and 20 wt.% GA have been reported elsewhere.[16] The range of firing temperature was adapted according to the previous studies, in which the DTA results revealed the surface crystallization of parent glasses and necessity of sintering above the crystallization temperatures of parent glasses.[17,18]

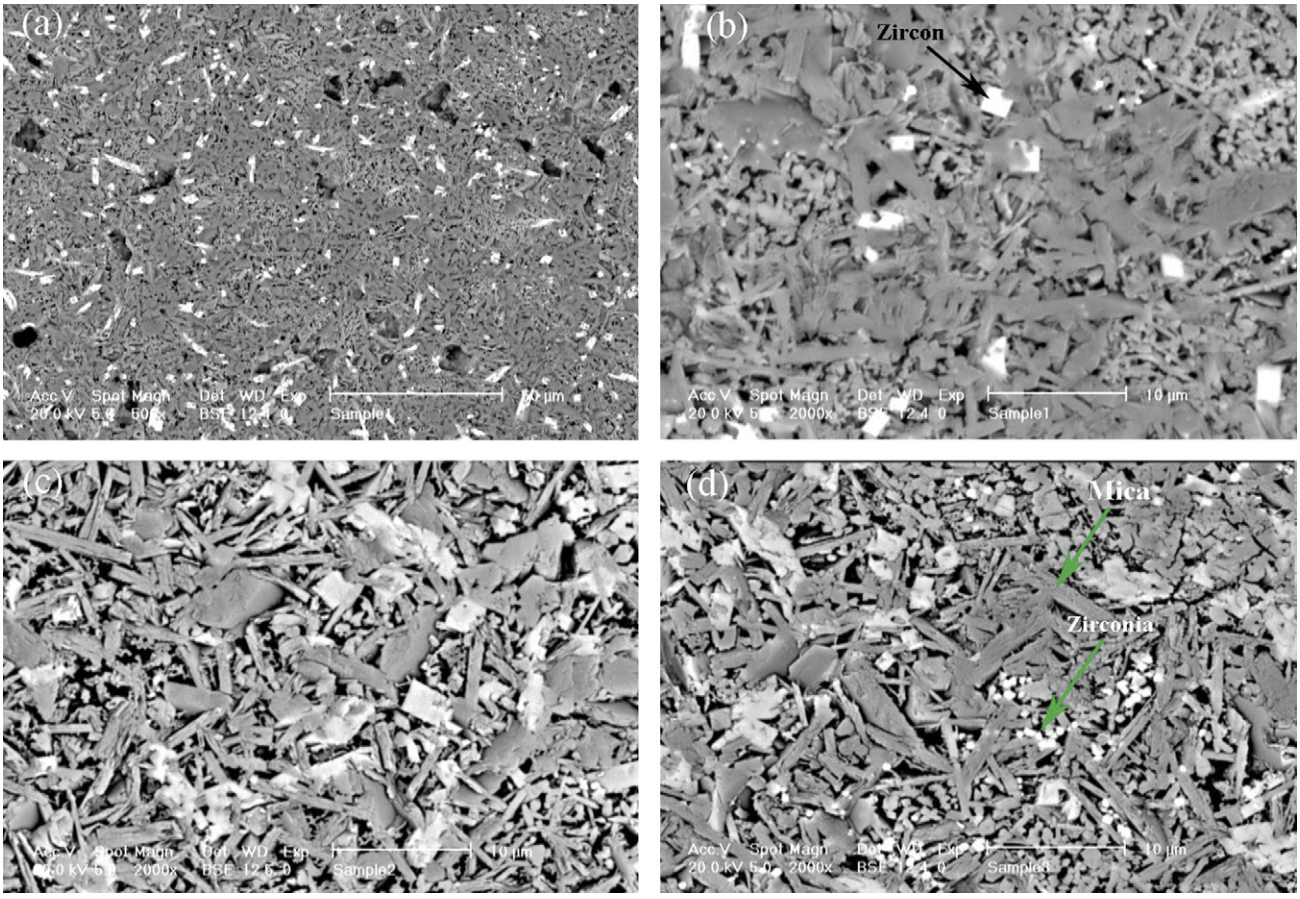

Fig. 3. SEM images of the composites: general view of C5Z (×500) (a) and C5Z (b), C10Z (c) and C15Z (d) (×2000).

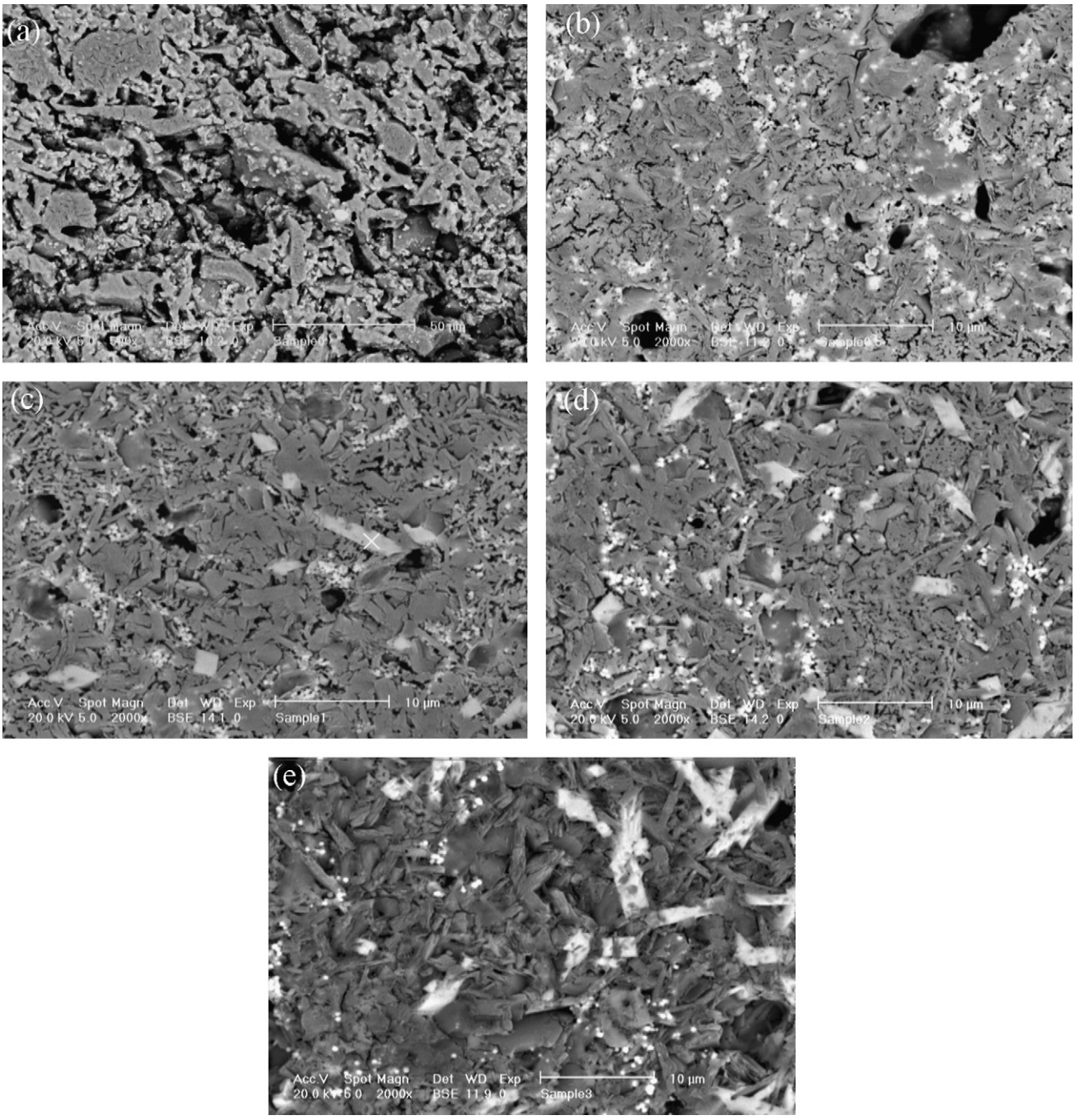

Fig. 5. Microstructures of the fired C10Z at various soaking times (×2000): 0 min (a), 30 min (b), 60 min (c), 120 min (d) and 180 min (e).

The relative density of composites and mica–apatite glass–ceramic versus temperature are plotted in Fig. 1. The optimum sintering temperature of samples was determined by considering the maximum relative density. Therefore, sintering temperatures of 1100, 1110, 1120 °C were chosen for C5Z, C10Z and C15Z, respectively. As it can be seen, adding Y-PSZ to the glass–ceramic matrix decreases the siterability and shifts the sintering temperatures to higher values. Bloating of the samples caused a decrease in the densities at the higher temperatures.

XRD patterns of the composites sintered at optimum temperatures are shown in Fig. 2. The sintered glass–ceramic contained fluorophlogopite, fluorapatite and minor amount of forsterite.[16] In addition to the mentioned phases presented in the glass–ceramic matrix, zircon ($ZrSiO_4$) and tetragonal zirconia (t-ZrO_2) were also detected in the composites. Relative intensity of t-ZrO_2 ($I_{(111)}$) in the composites to the silicon ($I_{(111)}$) was 0.14, 0.15 and 0.19 for C5Z, C10Z and C15Z, respectively.

The back-scattered SEM images of the sintered composite etched with 5 wt.% HF solution for 45 s are illustrated in Fig. 3. As can be seen, the microstructures of the sintered composites contain plate-like mica, elongated prismatic zircon crystals (with the ∼15–20 μm length and square basal plane of ∼2–3 μm

Table 2
Mechanical properties and relative density of specimens

Samples	Vickers micro-hardness (GPa)	Bending strength (MPa)	Fracture toughness (MPa $m^{1/2}$)	Relative density (%)
Mica–apatite glass–ceramic	3.25 ± 0.59	109.37 ± 18.31	0.85 ± 0.09	96.1
C5Z	3.45 ± 0.41	110.60 ± 23.39	1.23 ± 0.11	95
C10Z	4.48 ± 0.82	132.27 ± 14.30	1.44 ± 0.16	93.9
C15Z	4.35 ± 1.15	99.59 ± 10.67	1.38 ± 0.11	91.7

diagonal) as well as very fine (∼0.1 μm) spherical particles of zirconia. The phases are indicated by arrows on images. It has been shown that the excessive mutual diffusion of the two glasses at the glass–glass interfaces and/or unifying of them resulted in the formation of solid solution of K/Ca-mica and fluorapatite.[16] EDS analysis performed on the assumed prismatic zircon crystals (Fig. 4), which represents high content of silicon and zirconium, confirmed the composition of zircon. In a previous study, in which the mica glass–ceramic reinforced with Y-PSZ using the similar fluoro-mica glass, dissolution of Y-PSZ resulted in the formation of minor amount of zircon and transformed monoclinic zirconia (m-ZrO_2).[15] But, in this research almost the whole content of Y-PSZ were changed to the zircon due to the presence of second glass GA.

In order to investigate the consequence of phase formation in the composites, the prepared mixture of glass powders and 10 wt.% Y-PSZ (C10Z) was heated to the sintering temperature and remained for various times (i.e. 0, 30, 60, 120 and 180 min), then the samples immediately cooled. The SEM micrographs and XRD analyses of these samples corresponded to the soaking time are shown in Figs. 5 and 6, respectively. Fig. 5a represents the good dispersion of Y-PSZ powder in the glass matrix before the extensive commencement of sintering (viz. zero time), and at this time the glass–ceramic mainly contained initial Y-PSZ phase (80% t-ZrO_2 and 20% m-ZrO_2), forsterite and fluorapatite (Fig. 6). After 30 min mica nuclei formed and zirconia particles began to agglomerate between the initial glass powders, in order to reduce their free surface energy (Fig. 5b). The dissolution of the Y-PSZ was also observed in the residual glass (considering a dramatic decrease in the peak intensity of t-ZrO_2 in Fig. 6 at 30 min). By increasing the sintering time the prismatic zircon crystals began to crystallize gradually from the Zr- and Si-rich residual glass and mica crystals with interlocking structure finally formed (cf. Figs. 5c–e and 6). It should be noted that SiO_2 in the residual glass mainly supplied by glass GA, which just crystallized to the fluorapatite. Spherical zirconia particles can be also observed in Fig. 5d and e.

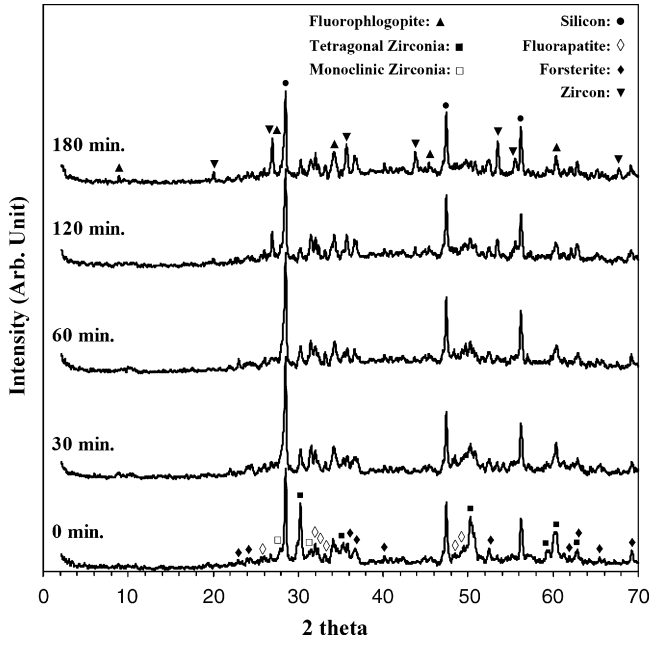

Fig. 6. XRD patterns of composite C10Z fired at different soaking times.

It can be concluded that zircon formation consists of three stages. First of all, Y-PSZ particles begin to agglomerate between the glass powders when the sintering process proceeds. The surface crystallization of mica glass and low viscosity of residual glass could enhance the agglomeration of the zirconia particles. Then, the Y-PSZ dissolves in the residual glass and finally the zircon precipitates in the residual glass during the final stage of sintering. It seems that, Y-PSZ dissolution and zircon formation strongly depends on the content of SiO_2 in the residual glass. In other words, it depends on the composition of the initial glasses. The addition of 20 wt.% GA to the GM would incorporate excess 4.95–5.53 wt.% silica (0.08–0.09 mole SiO_2) into the residual glass that could be enough to react with the whole content of 0.04 and 0.08 mole ZrO_2 in the composites C5Z and C10Z, respectively. Moreover, 0.08 mole ZrO_2 from the total amount of 0.12 in C15Z may react with 0.08 mole SiO_2 incorporated by GA. A comparison between the results of this study with the previous one[15] reveals that GM glass has a lower tendency to dissolve Y-PSZ when compared to the GA glass. Also, employing intense milling in the mixing stage would normally reduce the particle size of Y-PSZ and also increase the interfacial contact area between Y-PSZ particles and glasses; therefore it was expected to enhance the reactivity of Y-PSZ in the glass matrix. Nevertheless, a comparison between the two studies, in which a similar preparation process was used, revealed that the milling stage has little influence on the dissolution of Y-PSZ, since a minor amount of zircon was detected in the mica glass–ceramic composite.[15] In fact, the chemical composition of glass GA caused the nearly complete dissolution of Y-PSZ in this study, because it incorporated the excess SiO_2 into the residual glass. Above mentioned results, which correspond well with literature,[14,19,20] show that the reaction between zirconia and a glassy phase mainly depends on the chemical composition of the glass rather than the preparation method or firing schedule. Although, the fast firing process with minimum soaking time reduces the possibility of zircon formation, it would normally inhibit the full densification or

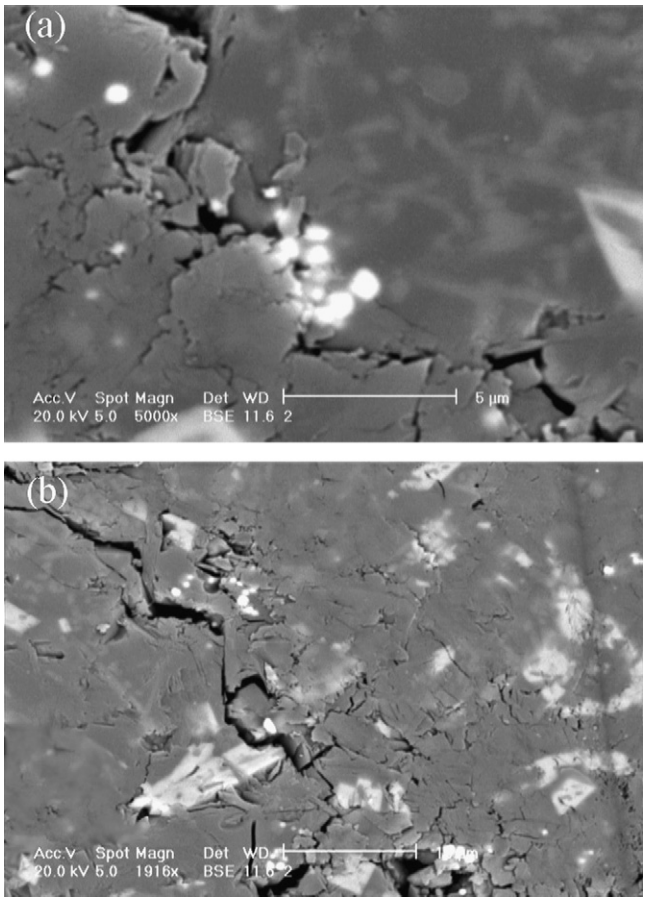

Fig. 7. Crack path induced by Vickers indentation on C10Z which passes through the zirconia agglomerate (a) and through the zircon crystal (b).

crystallization of the glass–ceramic. Fast firing process could be applicable for glazes.[14]

Mechanical properties as well as relative density of the sintered specimens are summarized in Table 2. All composites had a lower relative density than the mica–apatite glass–ceramic. The decrease in the relative density of composites could be due to the dissolution of ZrO_2 which leads to an increase in viscosity of the residual glass and interferes with further densification of composites via viscous flowing of the residual glass. Additionally, crystallization of zircon from the low density residual glass during the final stage of sintering incorporates further porosity into the matrix. Therefore composite C15Z which has the minimum relative density represent poor mechanical properties, although it has the maximum content of t-ZrO_2. C15Z shows the minimum bending strength and too much deviation in micro-hardness value due to the presence of high amount of porosity. Micro-hardness of composites generally increased because of the presence of hard zirconia and zircon crystals in the matrix. Although, too much change in strength values cannot be observed, the bending strength of the C10Z was the maximum value. Fracture toughness of the composites was also higher than the mica–apatite glass–ceramic. C15Z demonstrate lower toughness than the C10Z due to the lack of densification. Measurements show that C10Z has a best mechanical properties and it would be the optimum composition.

The increase in bending strength (except for C15Z) and fracture toughness of the composites can be attributed to the mechanisms such as crack deflection and transformation toughening by existing t-ZrO_2. Additionally, improved mechanical properties of composites may be arisen from the dissolution of Y-PSZ which caused the large share of Zr^{4+} ions in the form of complex $[ZrO_4]^{4-}$ structural units in the residual glass network unit.

Characteristic Vickers indentation crack for the composite C10Z in Fig. 7a and b shows propagating cracks which pass through the spherical zirconia agglomerate and zircon crystal, respectively. Crack deflection and also branching can be clearly observed in Fig. 7b. It seems that crack deflection can be related to the large mismatch in thermal expansion coefficient exists between $ZrSiO_4$, ZrO_2 crystals and glass–ceramic matrix. Moreover, it seems that transformation toughening has a little contribution to the increase of fracture toughness, since no significant increase was observed in the K_{IC} values of the composites in comparison with Mica–apatite glass–ceramic. The content of retained t-ZrO_2 is relatively low and even composite C15Z with maximum content of t-ZrO_2 has low fracture toughness.

The fracture surfaces of the mica–apatite glass–ceramic and C10Z are illustrated in Fig. 8a and b, respectively. As can be clearly observed, the fractured surface of C10Z is rougher

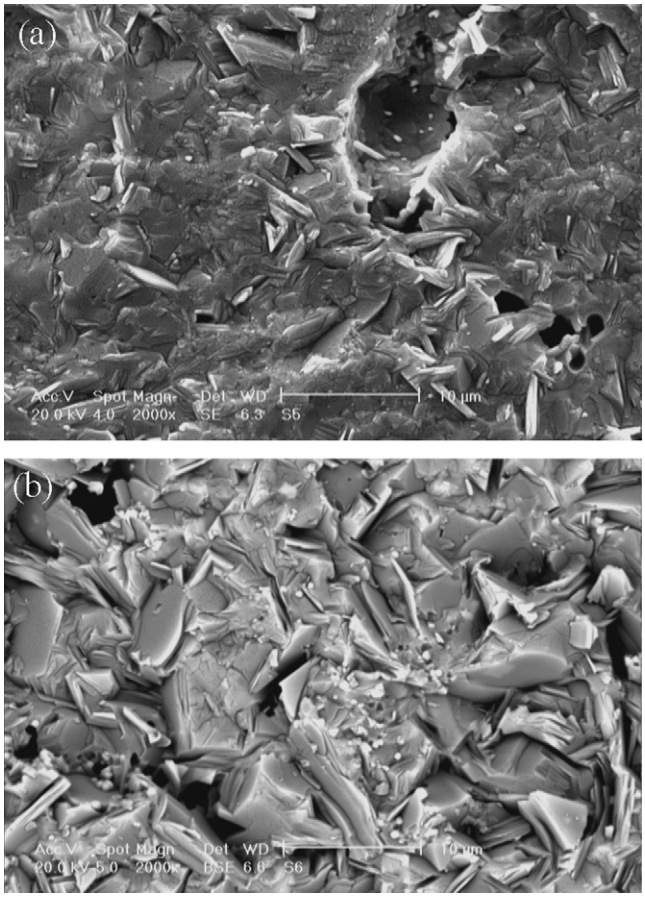

Fig. 8. SEM micrographs of fracture surfaces of the sintered specimens (×2000): mica–apatite glass–ceramic (a) and C10Z (b).

than the mica–apatite glass–ceramic. Too much cleavage plane of mica crystals around the fine zirconia particles in C10Z (Fig. 8a) shows that this fracture surface of the C10Z results from too much deflection of the propagating cracks. However, mica–apatite glass–ceramic represents few cleavage planes of the mica crystals which demonstrate a more brittle fracture than the C10Z.

4. Conclusions

1. Mica–apatite glass–ceramic matrix composites with suitable density were fabricated via pressureless sintering. Sintering was performed on the mixture of two mica- and apatite-based frits with various content of Y-PSZ.
2. Almost the whole content of Y-PSZ dissolved in the residual glass and resulted in the precipitation of zircon at the final stage of sintering. It seems that the dissolution of ZrO_2 merely depends on the chemical composition of apatite-based glass which incorporates excess silica into the residual glass. It was found that using ball-mill for mixing of Y-PSZ and initial glass powders has a little influence on the dissolution of Y-PSZ.
3. Mechanical properties of composite reinforced with 10 wt.% Y-PSZ improved in comparison with mica–apatite glass–ceramic. This can be attributed to crack deflection mechanism, which is arisen from the large mismatch in thermal expansion coefficient exists between $ZrSiO_4$ crystals and glass–ceramic matrix.

References

1. Höland, W. and Vogel, W., Machineable and phosphate glass–ceramics. In *An Introduction to Bioceramics*. In *Advances Series in Ceramics*, *Vol. 1*, ed. L. L. Hench and J. Wilson. World Scientific Publishing, 1993, pp.125–137.
2. Chen, X., Hench, L. L., Greenspan, D., Zhong, J. and Zhang, X., Investigation on phase separation, nucleation and crystallization in bioactive glass–ceramics containing fluorophlogopite and fluorapatite. *Ceram. Int.*, 1998, **24**, 401–410.
3. Höland, W. and Beall, G., *Glass–Ceramic Technology*. The American Ceramic Society, Westerville, OH, 2002, pp. 148–152.
4. Moisescu, C., Jana, C., Habelitz, S., Carl, G. and Rüssel, C., Oriented fluoroapatite glass–ceramics. *J. Non Cryst. Solids*, 1999, **248**, 176–182.
5. Xiang, Q., Liu, Y., Sheng, X. and Dan, X., Preparation of mica-based glass–ceramics with needle-like fluorapatite. *Dent. Mater.*, 2007, **23**, 251–258.
6. Taruta, S., Mukoyama, K., Suzuki, S. S., Kitajima, K. and Takusagawa, N., Crystallization process and some properties of calcium mica–apatite glass–ceramics. *J. Non Cryst. Solids*, 2001, **296**, 201–211.
7. Hench, L. L., Bioceramics. *J. Am. Ceram. Soc.*, 1998, **81**, 1705–1728.
8. Hannink, R. H. J., Kelly, P. M. and Muddle, B. C., Transformation toughening in zirconia-containing ceramics. *J. Am. Ceram. Soc.*, 2000, **83**, 461–487.
9. Verné, E., Defilippi, R., Carl, G., Vitale Brovarone, C. and Appendino, P., Viscous flow sintering of bioactive glass–ceramic composites toughened by zirconia particles. *J. Eur. Ceram. Soc.*, 2003, **23**, 675–683.
10. Kasuga, T., Nakajima, K., Uno, T. and Yoshida, M., Preparation of zirconia-toughened bioactive glass–ceramic composite sinter-hot isostatic pressing. *J. Am. Ceram. Soc.*, 1992, **75**, 1103–1107.
11. Choi, S. Y. and Ahn, J. M., Viscous sintering and mechanical properties of 3Y-TZP-reinforced LAS glass–ceramic composites. *J. Am. Ceram. Soc.*, 1997, **80**, 2982–2986.
12. McCoy, M. A. and Heuer, A. H., Microstructural characterization and fracture toughness of cordierite-ZrO_2 glass–ceramics. *J. Am. Ceram. Soc.*, 1988, **71**, 673–677.
13. Semar, W., Pannhorst, W., Hare, M. T. and Pulmour, H., Sintering of a crystalline cordierite/ZrO_2 composite. *Glastech. Ber.*, 1989, **62**, 74–78.
14. Llusar, M., Rodrigues, C., Labrincha, J., Flores, M. and Monrós, G., Reinforcement of single-firing ceramic glazes with the addition of polycrystalline tetragonal zirconia (3Y–TZP) or zircon. *J. Eur. Ceram. Soc.*, 2002, **22**, 632–652.
15. Montazerian, M., Alizadeh, P. and Eftekhari Yekta, B., Pressureless sintering and mechanical properties of mica glass–ceramic/Y-PSZ composite. *J. Eur. Ceram. Soc.*, 2008, **28**, 2687–2692.
16. Alizadeh, P., Eftekhari Yekta, B. and Javadi, T., Sintering behavior and mechanical properties of the mica-diopside machinable glass–ceramics. *J. Eur. Ceram. Soc.*, 2008, **28**, 1569–1573.
17. Eftekhari Yekta, B., Hashemi Nia, S. and Alizadeh, P., The effect of B_2O_3, PbO and P_2O_5 on the sintering and machinability of fluoromica glass–ceramics. *J. Eur. Ceram. Soc.*, 2005, **25**, 899–902.
18. Alizadeh, P., Eftekhari Yekta, B. and Gervei, A., Effect of Fe_2O_3 addition on the sinterability and machinability of glass–ceramics in the system MgO-CaO-SiO_2-P_2O_5. *J. Eur. Ceram. Soc.*, 2004, **24**, 3529–3533.
19. Castilone, R. J., Sriran, D., Carty, W. M. and Snyder, R. L., Crystallization of zircon in stoneware glazes. *J. Am. Ceram. Soc.*, 1999, **82**, 2819–2824.
20. Jacobs, C. W., Opacifying crystalline phases present in zirconium-type glazes. *J. Am. Ceram. Soc.*, 1954, **37**, 216–220.